

Liver X receptor activation promotes macrophage-to-feces reverse cholesterol transport in a dyslipidemic hamster model

François Briand,^{1,*} Morgan Tréguier,[†] Agnès André,^{*,†} Didier Grillot,[§] Marc Issandou,[§] Khadija Ouguerram,[†] and Thierry Sulpice^{*}

Physiogenex SAS,^{*} Prologue Biotech, Rue Pierre et Marie Curie, B.P. 28262, 31682 Labège-Innopole, France; Centre de Recherche en Nutrition Humaine-INSERM U915,[†] CHU Hôtel-Dieu, 8 quai Moncoussu B.P. 70721 44000 Nantes, France; and Biology Department,[§] GlaxoSmith Kline, Les Ulis Research Center, 15 avenue du Québec, 91951 Les Ulis, France

Abstract Liver X receptor (LXR) activation promotes reverse cholesterol transport (RCT) in rodents but has major side effects (increased triglycerides and LDL-cholesterol levels) in species expressing cholesteryl ester transfer protein (CETP). In the face of dyslipidemia, it remains unclear whether LXR activation stimulates RCT in CETP species. We therefore used a hamster model made dyslipidemic with a 0.3% cholesterol diet and treated with vehicle or LXR agonist GW3965 (30 mg/kg bid) over 10 days. To investigate RCT, radiolabeled ³H-cholesterol macrophages or ³H-cholesteryl oleate-HDL were then injected to measure plasma and feces radioactivity over 72 or 48 h, respectively. The cholesterol-enriched diet increased VLDL-triglycerides and total cholesterol levels in all lipoprotein fractions and strongly increased liver lipids. Overall, GW3965 failed to improve both dyslipidemia and liver steatosis. However, after ³H-cholesterol labeled macrophage injection, GW3965 treatment significantly increased the ³H-tracer appearance by 30% in plasma over 72 h, while fecal ³H-cholesterol excretion increased by 156% ($P < 0.001$). After ³H-cholesteryl oleate-HDL injection, GW3965 increased HDL-derived cholesterol fecal excretion by 64% ($P < 0.01$ vs. vehicle), while plasma fractional catabolic rate remained unchanged. Despite no beneficial effect on dyslipidemia, LXR activation promotes macrophage-to-feces RCT in dyslipidemic hamsters. These results emphasize the use of species with a more human-like lipoprotein metabolism for drug profiling.—Briand, F., M. Tréguier, A. André, D. Grillot, M. Issandou, K. Ouguerram, and T. Sulpice. Liver X receptor activation promotes macrophage-to-feces reverse cholesterol transport in a dyslipidemic hamster model. *J. Lipid Res.* 2010. 51: 763–770.

Supplementary key words cholesteryl ester transfer protein • lipoprotein • dyslipidemia • atherosclerosis

The liver X receptors (LXR; NR1H2/3) LXR α and LXR β are ligand-activated transcription factors of the nuclear receptor superfamily that control expression of genes involved in cholesterol homeostasis and fatty acid metabolism (1). In mice, activation of LXR has been shown to promote in vivo reverse cholesterol transport (RCT) (2, 3), a process by which cholesterol is effluxed from peripheral tissues to the liver for excretion into the bile and ultimately in the feces (4). Synthetic LXR ligands have been shown to stimulate cholesterol efflux from cultured macrophages (5, 6) and inhibit or even promote regression of atherosclerosis in mice (7, 8). Hence, studies performed in mice support LXR activation as an attractive target to prevent atherosclerosis (9).

However, concerns have been raised regarding undesired side effects such as liver steatosis, hypertriglyceridemia (10), and increased LDL-cholesterol levels in species, namely monkeys and hamsters, expressing cholesteryl ester transfer protein (CETP) (11). Despite these potentially harmful side effects, LXR agonists still represent a potential therapeutic target. For instance, indazole-based LXR modulators have been shown to reduce atherosclerosis and stimulation of hepatic triglyceride synthesis in mice and hamsters (12). Total cholesterol and LDL-cholesterol lowering effects have been recently shown in primates treated with one of those LXR modulators (13).

Although well characterized in rodents, it is actually unclear whether LXR activation would promote in vivo macrophage-to-feces RCT in species expressing CETP. This

Abbreviations: CETP, cholesteryl ester transfer protein; FCR, fractional catabolic rate; FGF19, fibroblast growth factor 19; HL, hepatic lipase; LCAT, lecithin:cholesteryl acyl transferase; LXR, liver X receptor; RCT, reverse cholesterol transport, PLTP, phospholipid transfer protein; SR-BI, scavenger receptor class B type I.

¹To whom correspondence should be addressed.
e-mail: f.briand@physiogenex.com

Manuscript received 23 October 2009 and in revised form 26 October 2009.

Published, JLR Papers in Press, October 27, 2009

DOI 10.1194/jlr.M001552

Copyright © 2010 by the American Society for Biochemistry and Molecular Biology, Inc.

This article is available online at <http://www.jlr.org>

represents an important preclinical issue before translating LXR therapies to humans, especially in the face of dyslipidemia. To address this question, we therefore developed a hamster model with both dyslipidemia and liver steatosis to assess the rate of RCT by injecting ^3H -cholesterol labeled macrophages *in vivo*. Because this experiment gives limited information regarding HDL metabolism, we combined this method with HDL-cholesteryl ester kinetics by injecting HDL- ^3H -cholesteryl oleate to better investigate the RCT process *in vivo*.

MATERIALS AND METHODS

Animals and diet

All animal protocols were approved by the local ethical committee (Comité regional d'éthique de Midi-Pyrénées). Male Golden Syrian hamsters (91–100 g, 6 weeks old) were housed in plastic cages (6–8 animals/cage) containing wood shavings and maintained in a room with a 12-h light cycle with free access to food and water. Animals were adapted to these conditions and fed a rodent chow diet (Purina chow #5001, Research Diets, NJ) for 1 week. This rodent chow diet was defined as the control diet.

Hamsters were then placed on either the control chow diet ($n = 8$) or a chow diet supplemented with 0.3% cholesterol ($n = 8$), pelleted from Research Diets, NJ. The diet was continued for 4 weeks and hamster body weight was monitored weekly. After 4 weeks of diet, hamsters were fasted overnight, blood glucose was monitored using a glucometer (Roche Diagnostics, Meylan, France), and a blood sample (1 ml) was collected by retro-orbital bleeding under isoflurane anesthesia. Animals were then euthanized by cervical dislocation, exsanguinated, and liver was harvested, weighed, flash-frozen in liquid nitrogen, and stored at -80°C until biochemical analysis.

In another experiment, hamsters were fed a cholesterol-enriched diet during 4 weeks and then treated orally for a total of 10 days with either vehicle (a saline solution of 0.5% hydroxypropyl methylcellulose, twice daily) or LXR agonist GW3965 (provided by GlaxoSmithKline, Les Ulis, France) 30 mg/kg, twice daily, as previously described (11). After 7–8 days of treatment, hamsters underwent *in vivo* macrophage-to-feces RCT or HDL-cholesteryl esters kinetics as described below.

Another group of hamsters fed the cholesterol-enriched diet were kept treated by vehicle ($n = 8$) or GW3965 ($n = 8$) until the end of the treatment period (10 days) to collect blood by retro-orbital bleeding (6 h postgavage, nonfasting conditions). Plasma was isolated and kept frozen at -80°C until biochemical analysis. After being euthanized by cervical dislocation, liver and the medium part (jejunum) of the small intestine were harvested. Jejunum segment was isolated using the 1:3:2 (duodenum-jejunum-ileum) lengths ratio method (14). Harvested tissues were weighed and flash-frozen in liquid nitrogen and then stored at -80°C until liver lipids assays. An aliquot of each tissue was also stored at -80°C in RNAlater (Invitrogen) for hepatic and intestinal gene expression.

Biochemical analysis

Total cholesterol, triglycerides, and free fatty acids were assayed using commercial kits (Biomerieux, Marcy l'Etoile, France; Wako Chemicals, Richmond, VA). HDL-cholesterol was determined using the phosphotungstate/ MgCl_2 precipitation method. Non-HDL cholesterol levels were then determined by subtracting HDL-cholesterol values from total plasma cholesterol. Plasma CETP, phospholipid transfer protein (PLTP), and

lecithin:cholesterol acyl transferase (LCAT) activities were measured by fluorescence using commercial kits (Roarbiomedical, New York, NY) as well as hepatic lipase (HL) activity (ProGen, Heidelberg, Germany). Fast protein liquid chromatography lipoprotein profiles (total cholesterol and triglycerides) using pooled plasma were performed as previously described (15). Hepatic cholesterol, triglycerides, and fatty acid levels were determined from liver homogenate incubated with deoxycholate (10).

RNA extraction and gene expression analysis

Tissue for mRNA analysis was homogenized, and RNA was isolated using Trizol reagent (Invitrogen) according to the manufacturer's instructions. Real-time quantitative PCR analysis was performed as follows: 1 μg of total RNA was reverse transcribed using 100 units of Moloney Murine Leukemia-Virus reverse transcriptase (Invitrogen). Real time quantitative PCR was performed on the 7000 Sequence Detection System with SYBR green MESAGREEN Master Mix Plus (Eurogentec, Angers, France). The reaction contained 10 ng of reverse transcribed total RNA, 500 nM forward and reverse primers, and 5 \times Sybr green Mix. Primer sequences are available on request. All reactions were performed at least in triplicate and cyclophilin RNA amplification was used as a reference. In all PCR assays and for each primer set, expression of a control cDNA was included as inter-run calibrator.

In vivo macrophage-to-feces RCT

Preparation of J774 cells and *in vivo* RCT study were performed as previously described (16) with minor modifications. J774 cells obtained from the American Type Culture Collection (Manassas, VA) were grown in suspension in RPMI/HEPES supplemented with 10% FBS and 0.5% gentamicin in suspension in Nalgene Teflon flasks. Cells were radiolabeled with 5 $\mu\text{Ci}/\text{ml}$ ^3H -cholesterol and cholesterol loaded with 50 $\mu\text{g}/\text{ml}$ oxidized LDL (kindly provided by Marine Goffinet from Cerenis Therapeutics) over 48 h. Radiolabeled cells were then washed with RPMI/HEPES and equilibrated for 4 h in fresh RPMI/HEPES supplemented with 0.2% BSA and gentamicin. Cells were pelleted by low speed centrifugation and resuspended in MEM/HEPES prior to injection into hamsters.

^3H -cholesterol-labeled and oxidized LDL-loaded J774 cells (2.5×10^6 cells containing 10×10^6 dpm in 0.5 ml minimum essential medium) were injected intraperitoneally into individually caged hamsters. Animals had free access to food and water and were treated twice daily with vehicle ($n = 6$) or LXR agonist GW3965 30 mg/kg twice daily ($n = 6$) over 72 h. Blood was collected by retro-orbital bleeding and under isoflurane anesthesia at 24, 48, and 72 h to measure radioactivity released into the plasma (10 μL counted in a liquid scintillation counter). Hamsters were then sacrificed by cervical dislocation and liver was harvested from each animal. An approximately 50 mg piece of liver was homogenized using an ultrasound probe in 500 μl water then 300 μl were counted in a liquid scintillation counter. Feces were collected over 72 h and were stored at 4°C before extraction of cholesterol and bile acid.

Fecal cholesterol and bile acid extraction was performed as previously described (16). The total feces collected from 0 to 72 h were weighed and soaked in Millipore water (1 ml water/100 mg feces) overnight at 4°C . The following day, an equal volume of absolute ethanol was added, and the mixtures were homogenized. To extract the ^3H -cholesterol and ^3H -bile acid fractions, 1 ml of the homogenized samples was combined with 1 ml ethanol and 200 μL NaOH. The samples were saponified at 95°C for 1 h and cooled to room temperature and then ^3H -cholesterol was extracted 2 times with 3 ml hexane. The extracts were pooled, evaporated, resuspended in toluene, and then counted in a liquid

scintillation counter. To extract ^3H -bile acids, the remaining aqueous portion of the feces was acidified with concentrated HCl and then extracted 2 times with 3 ml ethyl acetate. The extracts were pooled together, evaporated, resuspended in ethyl acetate, and counted in a liquid scintillation counter.

Results were expressed as a percent of the radioactivity injected recovered in plasma, liver, and feces. The plasma volume was estimated as 3.5% of the body weight.

In vivo ^3H -cholesteryl oleate-HDL kinetics

A plasma pool was obtained from normocholesterolemic hamsters maintained on a control diet. Hamster HDL ($d = 1.07\text{--}1.21$) were then isolated by ultracentrifugation as previously described (17). After extensive dialysis against saline, HDL were labeled with ^3H -cholesteryl oleate in the presence of lipoprotein deficient serum collected from rabbit plasma, as already described (17). The labeled HDL were reisolated by ultracentrifugation ($d = 1.07\text{--}1.21$) then extensively dialyzed prior injection.

The day before the in vivo experiment, catheters were inserted into the carotid artery (blood sampling) and into the jugular vein (injection) under isoflurane anesthesia. Catheters were kept patent with NaCl 0.9%. To prevent blood circulation and coagulation inside the catheter, a small volume of heparin (500 IU/ml) and glycerol (1 g/ml) was injected at the catheter extremity.

On the day of the experiment, hamsters were weighed and placed into individual cages. Animals had free access to food and water and were treated twice daily with vehicle ($n = 6$) or LXR agonist GW3965 30 mg/kg ($n = 6$) twice daily over 48 h. The ^3H -cholesteryl oleate-labeled HDL (≈ 2 million dpm) were injected intravenously and blood samples (150 μL) were collected at time $t = 5$ min, 1 h, 3 h, 6 h, 24 h, and 48 h after injection. Plasma was immediately centrifuged and stored at 4°C until radioactivity measurement in a liquid scintillation counter (10 μL plasma counted). Feces were collected over 48 h and were stored at 4°C before cholesterol and bile acids extraction, as described above.

Plasma decay curves were normalized to radioactivity at the initial 5 min time point after ^3H -cholesteryl oleate-labeled HDL injection. Plasma fractional catabolic rate (FCR) was then calculated from the area under the plasma disappearance curves fitted to a bicompartamental model using the SAAM II software.

Statistical analysis

Values are presented as mean \pm SEM. Comparisons between groups were conducted using the Student t -test (two-tailed). A two-tailed P -value of $P < 0.05$ was considered statistically significant.

RESULTS

Cholesterol-enriched diet induces dyslipidemia and hepatic steatosis in hamsters

Golden Syrian hamsters were fed a control chow or chow + 0.3% cholesterol diet for 4 weeks. As shown in **Table 1**, the chow + 0.3% cholesterol diet had no effect on body weight. However, there was a slight but significant 17% increase in blood glucose levels after an overnight fast ($P < 0.001$). The cholesterol-enriched diet increased total cholesterol plasma levels by 119% ($P < 0.001$). Both the HDL-cholesterol and non-HDL-cholesterol levels were increased (76 and 233%, respectively, $P < 0.001$ for both), which led to a 19% lower HDL-cholesterol-total cholesterol ratio ($P < 0.001$). Plasma triglycerides increased by 31% with the cholesterol-enriched diet ($P < 0.05$), while

TABLE 1. Body weight and plasma biochemical parameters after an overnight fast in hamsters fed a control chow or chow + 0.3% cholesterol diet over 4 weeks

	Chow	Chow + 0.3% Cholesterol
Body weight (g)	113.2 \pm 1.7	116.9 \pm 1.5
Fasted blood glucose (mg/dl)	82.5 \pm 3.0	96.0 \pm 2.4***
Total cholesterol (g/l)	1.31 \pm 0.06	2.87 \pm 0.10***
HDL-cholesterol (g/l)	0.95 \pm 0.05	1.67 \pm 0.11***
Non-HDL-cholesterol (g/l)	0.36 \pm 0.03	1.20 \pm 0.09***
HDL-cholesterol/total cholesterol	0.72 \pm 0.02	0.58 \pm 0.03***
Triglycerides (g/l)	1.06 \pm 0.05	1.39 \pm 0.12*
Free fatty acids (mmol/l)	0.66 \pm 0.07	0.68 \pm 0.04
CETP activity (pmol/h/ μL)	5.37 \pm 0.36	7.14 \pm 0.61**
PLTP activity (pmol/min/ μL)	0.75 \pm 0.02	1.36 \pm 0.02***
LCAT activity (AU)	7.74 \pm 0.13	8.39 \pm 0.13**
HL activity (pmol/min/ml)	3.66 \pm 0.14	3.96 \pm 0.31

Mean \pm SEM, $n = 8$ per group, * $P < 0.05$, ** $P < 0.01$, *** $P < 0.001$ vs. chow.

free fatty acids remained unchanged. The cholesterol-enriched diet increased CETP, PLTP, and LCAT activity by 33, 81, and 8%, respectively ($P < 0.01$ for all). There was no change regarding HL activity.

The diet-induced dyslipidemia was confirmed with lipoprotein cholesterol profiles analyzed by fast protein liquid chromatography (pooled plasma from overnight fasted hamsters), with higher total cholesterol levels in VLDL, LDL, and HDL fractions (**Fig. 1A**) as well as higher VLDL-triglycerides (**Fig. 1B**). No change was detectable regarding LDL and HDL-triglycerides. Moreover, liver harvested after 4 weeks of diet showed a 66% increase in organ weight (0.027 ± 0.001 vs. 0.045 ± 0.001 g/g body weight, $P < 0.001$, data not shown). As shown in **Fig. 1C**, chow + 0.3% cholesterol diet strongly increased hepatic cholesterol, triglycerides, and fatty acids by 535, 168, and 437%, respectively ($P < 0.001$ for all).

Overall, these data indicate that chow + 0.3% cholesterol diet provided over 4 weeks induces dyslipidemia and liver steatosis in golden Syrian hamsters.

LXR agonist GW3965 fails to improve dyslipidemia and hepatic steatosis in hamsters fed a cholesterol-enriched diet

We then investigated the effects of the LXR agonist GW3965 (30 mg/kg twice daily) in hamsters fed the chow + 0.3% cholesterol diet. After 10 days of treatment, blood was collected 6 h after drug dosing (nonfasting conditions) to assay plasma lipids. As shown in **Table 2**, there was a slight 11% decrease in total cholesterol ($P < 0.05$ vs. vehicle). There was a similar trend for HDL-cholesterol levels, although the 17% decrease did not reach significance ($P = 0.06$). When lipoprotein profiles were performed (pooled plasma from nonfasted hamsters), the decrease in HDL-cholesterol was more evident, while total cholesterol levels were slightly lower in LDL fractions (**Fig. 2A**). Meanwhile, calculated non-HDL-cholesterol and the HDL-cholesterol-total cholesterol ratio remained unchanged (**Table 2**). The main effect of GW3965 on plasma lipids was a significant 52% increase in plasma triglycerides (**Table 2**). This increased was seen in only the VLDL

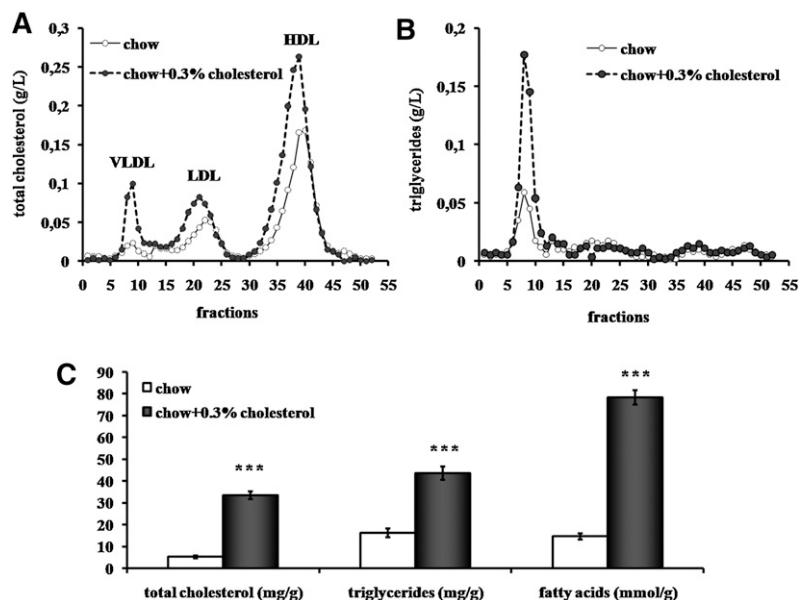


Fig. 1. Impact of cholesterol enriched diet on plasma and hepatic lipid content. Distribution of cholesterol (A) and triglycerides (B) in the plasma of overnight fasted hamsters after a 4 week chow diet or chow + 0.3% cholesterol analyzed by gel filtration chromatography (pooled plasma). (C) Hepatic total cholesterol, triglycerides, and fatty acid levels per gram wet weight in hamsters fed a 4 week chow (open bars) or chow + 0.3% cholesterol (solid bars) diet. Values are means \pm SEM (n = 8 per group, *** $P < 0.001$ vs. chow fed hamsters).

fractions (Fig. 2B). Treatment with GW3965 increased CETP activity by 22% (measured at 6 h postdosing), but not significantly (Table 2). There was no significant effect on liver total cholesterol, triglycerides, or fatty acids (Fig. 2C). Except for VLDL-triglycerides, these data suggest that LXR activation with GW3965 has no major effects on plasma and liver lipids in dyslipidemic hamsters.

LXR agonist GW3965 has significant effects on genes involved in cholesterol metabolism

The effects of LXR agonist GW3965 on liver and intestine gene expression are shown in Fig. 3. In the liver (Fig. 3A), there was a 69, 164, and 878% increase in ATP binding cassette protein A1, G5, and G8 mRNA expression, respectively ($P < 0.001$ vs. vehicle for all), while G1 expression was unexpectedly decreased by 74% with GW3965 treatment ($P < 0.001$). The reason for this lower hepatic ABCG1 expression remains unclear. Expression of cholesterol 7α -hydroxylase A1 was 85% lower as well ($P < 0.001$). The ACAT2 expression increased by 56% ($P < 0.001$). As expected, a huge 1551% increase in hepatic sterol-regulatory element binding protein 1c expression was observed with GW3965 treatment ($P < 0.001$). As shown in Fig. 3B, the same effect was seen in the intestine (2117% increase, $P < 0.001$). The expected effect of GW3965 on ATP binding cassette protein A1 and G1 intestinal expression

was observed (1235 and 2551% increase, respectively, $P < 0.001$ for both). Effects of LXR activation on genes involved in intestinal cholesterol absorption were also observed with a 159 and 105% increase in ABCG5 and G8 mRNA expression, respectively ($P < 0.001$ for both), while Niemann Pick C1-Like 1 expression was decreased by 34% ($P < 0.02$). No effect was seen on ACAT2 expression. These data indicate that LXR agonist GW3965 has significant effects on the expression of genes involved in cholesterol metabolism.

LXR agonist GW3965 promotes macrophage-to-feces RCT in dyslipidemic hamsters in vivo

To investigate whether LXR activation promotes RCT, radiolabeled macrophages were injected in dyslipidemic hamsters treated with vehicle or LXR agonist GW3965. As shown in Fig. 4A, plasma tracer appearance was $\sim 30\%$ higher in hamsters treated with the LXR agonist at 24 h ($P < 0.01$ vs. vehicle), 48 h, and 72 h ($P < 0.05$ for both) after injection. As shown in Fig. 4B, ^3H -tracer recovery was 27% higher in the liver of hamsters treated with GW3965 at 72 h ($P < 0.05$). The ^3H -tracer recovery was also measured in feces after chemical extraction (Fig. 4C). Interestingly, there was a significant 156% increase in the ^3H -free sterols fecal excretion for hamsters treated with the LXR agonist GW3965. No significant change was seen in the bile acids fraction. Overall, these data show that LXR activation promotes macrophage-to-feces RCT in dyslipidemic hamsters in vivo.

LXR agonist GW3965 promotes HDL-derived fecal cholesterol excretion despite no effect on plasma FCR

To test whether LXR agonist GW3965 affects HDL metabolism and HDL-derived cholesterol fecal excretion, hamsters were then injected with ^3H -cholesteryl oleate-labeled HDL. As shown in Fig. 5A, GW3965 had no effect on plasma decay curve. Expectedly, plasma FCR, calculated with the SAAMII software, remained unchanged (Fig. 5A). Free sterols and bile acids were extracted from feces

TABLE 2. Plasma lipids in nonfasted hamsters fed a chow + 0.3% cholesterol diet after 10 days of treatment with vehicle or LXR agonist GW3965 twice daily

	Vehicle	GW3965
Total cholesterol (g/l)	3.33 \pm 0.14	2.95 \pm 0.13*
HDL-cholesterol (g/l)	2.19 \pm 0.05	1.82 \pm 0.11
Non-HDL-cholesterol (g/l)	1.14 \pm 0.17	1.14 \pm 0.22
HDL-cholesterol/total cholesterol	0.66 \pm 0.02	0.62 \pm 0.03
Triglycerides (g/l)	0.97 \pm 0.05	1.48 \pm 0.12*
CETP activity (pmol/h/ μl)	10.0 \pm 1.41	12.2 \pm 0.93

Mean \pm SEM, n = 8 per group, * $P < 0.05$ vs. vehicle.

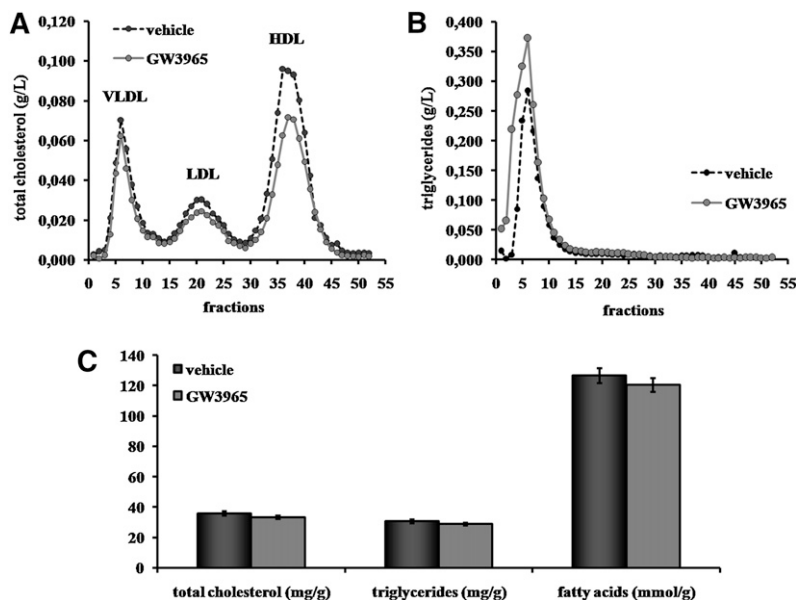


Fig. 2. Effect of GW3965 LXR agonist on plasma and liver lipid content. Hamsters on a chow + 0.3% cholesterol diet were orally dosed twice daily for 10 days with vehicle (0.5% hydroxypropyl methylcellulose) or GW3965 (30 mg/kg). Distribution of total cholesterol (A) and triglycerides (B) in the plasma of nonfasted hamsters treated or not with GW3965 were analyzed (6 h postgavage, pooled plasma). (C) Hepatic total cholesterol, triglycerides, and fatty acids levels per gram wet weight in hamsters treated with vehicle (solid bars) or with GW3965 (gray bars) were estimated. Values are means \pm SEM ($n = 8$ per group).

collected over 48 h after tracer injection. As shown in Fig. 5B, GW3965 significantly increased by 64% fecal free sterols excretion ($P < 0.01$). There was no change in fecal bile acids. These data indicate that LXR activation has no effect on plasma FCR but promotes HDL-derived cholesterol fecal excretion in dyslipidemic hamsters *in vivo*.

DISCUSSION

The present results demonstrate that LXR activation with GW3965 promotes macrophage-to-feces RCT in a hamster model with both dyslipidemia and liver steatosis. Because plasma FCR after ^3H -cholesteryl oleate-labeled HDL injection was not changed, LXR activation likely had major effects on macrophage cholesterol efflux, biliary cholesterol excretion, and inhibition of intestinal cholesterol absorption. Overall, this led to an enhanced mac-

rophage- and HDL-derived cholesterol fecal excretion, which respectively increased by 156 and 64%.

To better perform preclinical profiling of compounds affecting RCT (e.g., LXR agonists), we aimed to develop a nutritional model with a similar lipoprotein metabolism compared with humans. Among small animals, the hamster does express CETP and HL, which potentially forms small dense LDL (18), and has no hepatic apolipoprotein B48 production (19). Thus, the hamster has been useful to test the effects of CETP inhibition (20), activation of LXR (21, 11), farnesoid X receptor (22), and peroxisome proliferator activated receptor α (23) on lipoprotein metabolism. Moreover, hamsters easily develop dyslipidemia when fed an atherogenic diet (23, 24) and insulin resistant/diabetic states can be reached when diets are supplemented with fructose (25) or high percentage of fat (23). In the present study, a chow+0.3% cholesterol diet was used to mainly induce dyslipidemia with limited effects on

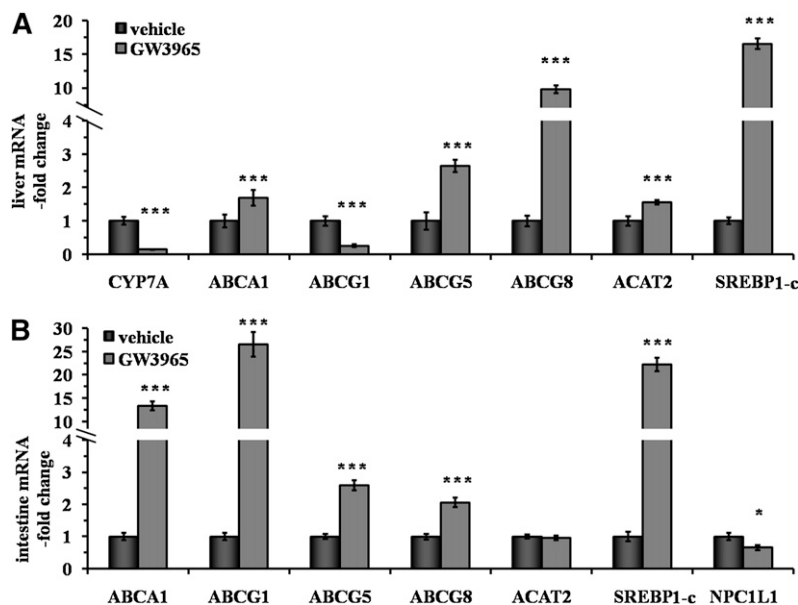


Fig. 3. Impact of LXR agonist on gene expression in liver and intestine. Hamsters on a chow + 0.3% cholesterol diet were orally dosed twice daily for 10 days with vehicle (0.5% hydroxypropyl methylcellulose) or GW3965 (30 mg/kg). Gene expression was measured by real-time quantitative PCR in liver (A) and intestine (B) in both vehicle (solid bars) and GW3965 (gray bars) groups. Values are means \pm SEM ($n = 8$ per group, * $P < 0.05$; *** $P < 0.001$ vs. vehicle).

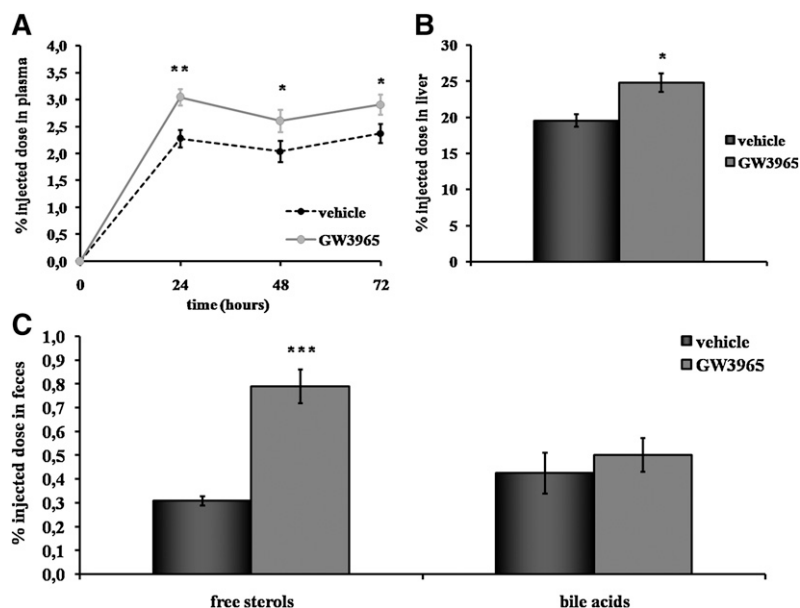


Fig. 4. Effects of GW3965 LXR agonist on macrophage-to-feces RCT. Hamsters on a chow + 0.3% cholesterol diet were orally treated twice daily for 7 days with vehicle (0.5% hydroxypropyl methylcellulose) or GW3965 (30 mg/kg) and then injected with ^3H -cholesterol labeled macrophages. Animals were treated with vehicle or GW3965 during the 72 h experiment. Time course of ^3H -cholesterol distribution in plasma of hamsters of each group was established (A) after injection of radiolabeled macrophages. Liver (B) and fecal (C) ^3H -tracer recovery in hamsters of vehicle group (solid bars) and GW3965 group (gray bars) were also monitored. Data are expressed as percent of dpm injected \pm SEM ($n = 6$ per group, * $P < 0.05$; ** $P < 0.01$; *** $P < 0.001$ vs. vehicle).

insulin resistance/diabetes. As expected, hamsters fed a chow + 0.3% cholesterol diet had a significant decrease in the HDL-cholesterol-total cholesterol ratio and increased triglycerides levels as well as CETP activity.

Based on our hamster model, we then investigated whether LXR activation affects lipoprotein metabolism and RCT in light of the metabolic disorders aforementioned. As previously described in normal hamsters (11), the main GW3965 side effect was the increased plasma triglyceride levels, a likely consequence of the strong increase in sterol-regulatory element binding protein 1c mRNA expression seen in both liver and intestine. Despite the increase in VLDL-triglycerides, it is likely that other LXR side effects (increased LDL-cholesterol and CETP activity) have been partly offset by the dyslipidemic state already induced upon the 0.3% cholesterol diet. Very recent

studies in hamsters have suggested that metabolic disturbance induced by dietary cholesterol might be related to LXR activation (25). One might also speculate that the 0.3% cholesterol might increase LDL-cholesterol levels through a lower hepatic LDL-receptor expression, because LXR has been shown to induce the E3 ubiquitin ligase Inducible Degradator of the LDLR in mice (26). Interestingly, treatment with the LXR agonist TO901317 in hamster dysregulates hepatic insulin signaling, which dramatically leads to higher triglyceride-rich VLDL particles production (27). The present data suggest that similar effects may have occurred in our hamster model.

Because biochemical parameters (e.g., HDL-cholesterol levels) are not fully predictive regarding the rate of RCT, we then used a combination of in vivo RCT and HDL-cholesterol ester kinetic experiments. Despite the maintained

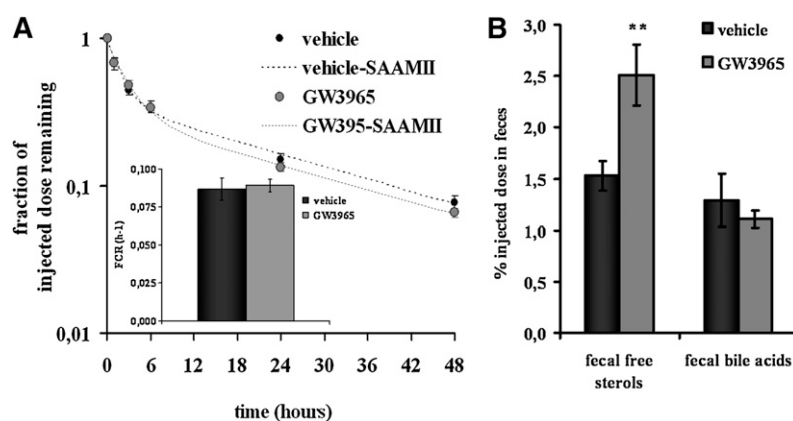


Fig. 5. Effects of GW3965 LXR agonist on HDL-cholesteryl esters kinetics and HDL-derived fecal cholesterol excretion. Hamsters on a chow + 0.3% cholesterol diet were orally treated twice daily for 8 days with vehicle (0.5% hydroxypropyl methylcellulose) or GW3965 (30 mg/kg) and then injected with ^3H -cholesteryl oleate labeled HDL. Animals were treated with vehicle or GW3965 during the 48 h experiment. After injection of radiolabeled HDL, plasma decay curves (A) of vehicle- (solid plots) and GW3965-treated hamsters (gray plots) were analyzed and fitted curves (dashed line) and FCR were calculated by SAAMII software. Fecal ^3H tracer recovery (B) were detected in hamsters treated with vehicle (solid bars) or GW3965 LXR agonist (gray bars). Values are means \pm SEM ($n = 6$ per group, ** $P < 0.01$ vs. vehicle).


or somewhat aggravated dyslipidemic state, LXR activation with GW3965 significantly promoted macrophage-to-feces RCT in vivo. After radiolabeled macrophage injection, the first stimulated step by LXR activation was likely the macrophage cholesterol efflux, which led to the ~30% increase in ^3H -cholesterol plasma appearance at all time points. This increase was not related to a lower removal of cholesteryl esters originally contained in HDL, because plasma FCR remained unchanged upon LXR activation. One might also speculate that more cholesterol effluxed from the macrophage reached the liver for further excretion into the bile rather than accumulation in hepatocyte. Actually, ABCG5 and G8, known targets of LXR (28), were strongly increased and may have directly promoted biliary cholesterol excretion, as described in mice (29). Besides increased biliary cholesterol excretion, inhibition of intestinal cholesterol absorption might have been the other crucial mechanism for promoting macrophage- and HDL-derived cholesterol fecal excretion. Recently, inhibiting intestinal cholesterol absorption in mice with ezetimibe (16, 30) or PPAR δ agonist (16) has been shown to promote macrophage-to-feces RCT. In mice, activation of LXR reduces intestinal cholesterol absorption, because intestinal ABCG5/G8 (28, 29) and Niemann Pick C1-Like 1 (31) are targeted by LXR as well. In the present study, similar effects were found upon GW3965 treatment, which would have contributed to reduce intestinal reabsorption of macrophage- and HDL-derived cholesterol.

Although biliary excretion and intestinal absorption may have been the main contributors to higher cholesterol fecal excretion, LXR agonist GW3965 could have stimulated a novel pathway for RCT, namely transintestinal cholesterol excretion (32). This nonbiliary route, which mediates the direct cholesterol excretion from plasma to the intestinal lumen, has been shown to be stimulated by LXR activation in Mdr2 knock-out mice, a model of biliary cholesterol excretion deficiency (33). To address whether this occurs in hamsters, quantification of this nonbiliary route would require more invasive experiments, such as intestine perfusion procedures, as described elsewhere (34, 35).

Another new mechanistic issue was suggested by the lower CYP7A mRNA hepatic expression upon LXR agonist GW3965 treatment. Recently, Quinet et al. (13) showed a transcriptional activation of the gene encoding primate fibroblast growth factor 19 (FGF19) with a synthetic LXR modulator, which may repress CYP7A expression. FGF19 has been shown to increase metabolic rate and reverse both dietary and leptin-deficient diabetes (36). Although we did not measure FGF19 expression in the present study (yet no literature exists regarding a hamster homolog of FGF19), this highlights new potential mechanistic insights to prevent atherosclerosis related to metabolic disease with LXR activation.

From a methodological point of view, we performed both ^3H -cholesterol labeled macrophage and ^3H -cholesteryl oleate labeled HDL injection to better investigate the macrophage-to-feces RCT pathway. Although we did not use hamster macrophages (a reduced number of murine J774 cells was injected to limit inflammation), injection of

radiolabeled macrophages demonstrated that the overall RCT from the macrophage to the feces is stimulated by LXR. However, the pathway of cholesterol from HDL in the plasma to the feces was more highlighted by the HDL-cholesteryl esters kinetics. Although we did not discriminate the direct (scavenger receptor class B type I pathway) and indirect (CETP pathway) routes of hamster RCT, HDL substantially gave useful information regarding the potent effects of LXR on HDL-cholesterol metabolism. Given that the plasma FCR remained unchanged after ^3H -cholesteryl oleate labeled HDL injection, increased ^3H -tracer plasma appearance after radiolabeled macrophage injection seems more related to an upregulated macrophage cholesterol efflux rather than a lower ^3H -cholesterol removal from the plasma. After ^3H -cholesteryl oleate HDL injection, the higher ^3H -cholesterol fecal excretion also indicated that HDL-derived cholesterol may be excreted more into the bile and reabsorbed less by the intestine with LXR activation. With the use of CETP species that more closely reflects human lipoprotein metabolism, both of these in vivo experiments may better reveal the mechanisms occurring with a given compound in humans. Hence, radiotracer-based methods should be combined with plasma biochemical parameters, which remain less predictive regarding RCT, as suggested in the present study (e.g., trend to lower HDL-cholesterol levels but increased rate of RCT).

In conclusion, the present data demonstrate that LXR agonist GW3965 promotes macrophage-to-feces RCT in dyslipidemic hamsters in vivo. These results suggest that LXR agonists would be likely to promote RCT in humans with dyslipidemia and emphasizes the relevance of LXR as a therapeutic target. In this goal, LXR modulators with favorable pharmacological profiles, as recently shown in hamsters and primates (13), still represent a potential therapy to treat cardiovascular diseases. 

The authors are indebted to Matthieu Bringart, Cécile Molveaux, and Quentin Thiéblemont (Physiogenex) for their expertise in animal surgery and technical assistance. The authors are also indebted to Marc Dubourdeau and Gérald Chêne (Ambiotis) as well as Rudi Baron, Marine Goffinet, and Nadia Boubekeur (Cerenis Therapeutics) for their help in J774 cells culture.

REFERENCES

1. Fiévet, C., and B. Staels. 2009. Liver X receptor modulators: effects on lipid metabolism and potential use in the treatment of atherosclerosis. *Biochem. Pharmacol.* **77**: 1316–1327.
2. Naik, S. U., X. Wang, J. S. Da Silva, M. Jaye, C. H. Macphee, M. P. Reilly, J. T. Billheimer, G. H. Rothblat, and D. J. Rader. 2006. Pharmacological activation of liver X receptors promotes reverse cholesterol transport in vivo. *Circulation.* **113**: 90–97.
3. Calpe-Berdiel, L., N. Rotllan, C. Fiévet, R. Roig, F. Blanco-Vaca, and J. C. Escolà-Gil. 2008. Liver X receptor-mediated activation of reverse cholesterol transport from macrophages to feces in vivo requires ABCG5/G8. *J. Lipid Res.* **49**: 1904–1911.
4. Rader, D. J., E. T. Alexander, G. L. Weibel, J. Billheimer, and G. H. Rothblat. 2009. The role of reverse cholesterol transport in animals and humans and relationship to atherosclerosis. *J. Lipid Res.* **50**(Suppl): S189–S194.
5. Repa, J. J., and D. J. Mangelsdorf. 2002. The liver X receptor gene team: potential new players in atherosclerosis. *Nat. Med.* **8**: 1243–1248.

6. Wang, N., M. Ranalletta, F. Matsuura, F. Peng, and A. R. Tall. 2006. LXR-induced redistribution of ABCG1 to plasma membrane in macrophages enhances cholesterol mass efflux to HDL. *Arterioscler. Thromb. Vasc. Biol.* **26**: 1310–1316.
7. Joseph, S. B., E. McKilligin, L. Pei, M. A. Watson, A. R. Collins, B. A. Laffitte, M. Chen, G. Noh, J. Goodman, G. N. Hagger, et al. 2002. Synthetic LXR ligand inhibits the development of atherosclerosis in mice. *Proc. Natl. Acad. Sci. USA.* **99**: 7604–7609.
8. Levin, N., E. D. Bischoff, C. L. Daige, D. Thomas, C. T. Vu, R. A. Heyman, R. K. Tangirala, and I. G. Schulman. 2005. Macrophage liver X receptor is required for antiatherogenic activity of LXR agonists. *Arterioscler. Thromb. Vasc. Biol.* **25**: 135–142.
9. Rader, D. J. 2007. Liver X receptor and farnesoid X receptor as therapeutic targets. *Am. J. Cardiol.* **100**: n15–19.
10. Miao, B., S. Zondlo, S. Gibbs, D. Cromley, V. P. Hosagrahara, T. G. Kirchgessner, J. Billheimer, and R. Mukherjee. 2004. Raising HDL cholesterol without inducing hepatic steatosis and hypertriglyceridemia by a selective LXR modulator. *J. Lipid Res.* **45**: 1410–1417.
11. Groot, P. H., N. J. Pearce, J. W. Yates, C. Stocker, C. Sauermeier, C. P. Doe, R. N. Willette, A. Olzinski, T. Peters, D. d'Epagnier, et al. 2005. Synthetic LXR agonists increase LDL in CETP species. *J. Lipid Res.* **46**: 2182–2191.
12. Wrobel, J., R. Steffan, S. M. Bowen, R. Magolda, E. Matelan, R. Unwalla, M. Basso, V. Clerin, S. J. Gardell, P. Nambi, et al. 2008. Indazole-based liver X receptor (LXR) modulators with maintained atherosclerotic lesion reduction activity but diminished stimulation of hepatic triglyceride synthesis. *J. Med. Chem.* **51**: 7161–7168.
13. Quinet, E.M., M.D. Basso, A.R. Halpern, D.W. Yates, R.J. Sheffan, V. Clerin, C. Resmini, J.C. Keith, T.J. Berrodin et al. 2009. LXR ligand lowers LDL cholesterol in primates, is lipid neutral in hamster, and reduces atherosclerosis in mouse. *J. Lipid Res.* **50**: 2358–2370.
14. Duan, L. P., H. H. Wang, A. Ohashi, and D. Q. Wang. 2006. Role of intestinal sterol transporters Abcg5, Abcg8, and Npc111 in cholesterol absorption in mice: gender and age effects. *Am. J. Physiol. Gastrointest. Liver Physiol.* **290**: G269–G276.
15. Briand, F., T. Magot, M. Krempf, P. Nguyen, and K. Ouguerram. 2006. Effects of atorvastatin on high-density lipoprotein apolipoprotein A-I metabolism in dogs. *Eur. J. Clin. Invest.* **36**: 224–230.
16. Briand, F., S. U. Naik, I. Fuki, J. S. Millar, C. MacPhee, M. Walker, J. Billheimer, G. Rothblat, and D. J. Rader. 2009. Both the peroxisome proliferator-activated receptor δ agonist, GW0742, and ezetimibe promote reverse cholesterol transport in mice by reducing intestinal reabsorption of HDL-derived cholesterol. *Clin. Trans. Sci.* **2**: 127–133.
17. Woollett, L. A., and D. K. Spady. 1997. Kinetic parameters for high density lipoprotein apoprotein AI and cholesteryl ester transport in the hamster. *J. Clin. Invest.* **99**: 1704–1713.
18. Lewis, G. F., S. Murdoch, K. Uffelman, M. Naples, L. Szeto, A. Albers, K. Adeli, and J. D. Brunzell. 2004. Hepatic lipase mRNA, protein, and plasma enzyme activity is increased in the insulin-resistant, fructose-fed Syrian golden hamster and is partially normalized by the insulin sensitizer rosiglitazone. *Diabetes.* **53**: 2893–2900.
19. Liu, G. L., L. M. Fan, and R. N. Redinger. 1991. The association of hepatic apoprotein and lipid metabolism in hamsters and rats. *Comp. Biochem. Physiol. A Comp. Physiol.* **99**: 223–228.
20. Tchoua, U., W. D'Souza, N. Mukhamedova, D. Blum, E. Niesor, J. Mizrahi, C. Maugeais, and D. Sviridov. 2008. The effect of cholesteryl ester transfer protein overexpression and inhibition on reverse cholesterol transport. *Cardiovasc. Res.* **77**: 732–739.
21. Schultz, J. R., H. Tu, A. Luk, J. J. Repa, J. C. Medina, L. Li, S. Schwendner, S. Wang, M. Thoolen, D. J. Mangelsdorf, et al. 2000. Role of LXRs in control of lipogenesis. *Genes Dev.* **14**: 2831–2838.
22. Bilz, S., V. Samuel, K. Morino, D. Savage, C. S. Choi, and G. I. Shulman. 2006. Activation of the farnesoid X receptor improves lipid metabolism in combined hyperlipidemic hamsters. *Am. J. Physiol. Endocrinol. Metab.* **290**: E716–E722.
23. Wang, P. R., Q. Guo, M. Ippolito, M. Wu, D. Milot, J. Ventre, T. Doebber, S. D. Wright, and Y. S. Chao. 2001. High fat fed hamster, a unique animal model for treatment of diabetic dyslipidemia with peroxisome proliferator activated receptor alpha selective agonists. *Eur. J. Pharmacol.* **427**: 285–293.
24. Basciano, H., A. E. Miller, M. Naples, C. Baker, R. Kohen, E. Xu, Q. Su, E. Allister, M. Wheeler et al. 2009. Metabolic effects of dietary cholesterol in an animal model of insulin resistance and hepatic steatosis. *Am. J. Physiol. Endocrinol. Metab.* **297**: E462–473.
25. Hsieh, J., A. A. Hayashi, J. Webb, and K. Adeli. 2008. Postprandial dyslipidemia in insulin resistance: mechanisms and role of intestinal insulin sensitivity. *Atheroscler. Suppl.* **9**: 7–13.
26. Zelcer, N., C. Hong, R. Boyadjian, and P. Tontonoz. 2009. LXR regulates cholesterol uptake through idol-dependent ubiquitination of the LDL receptor. *Science.* **325**: 100–104.
27. Basciano, H., A. E. Miller, C. Baker, M. Naples and K. Adeli. 2009. LXR alpha activation perturbs hepatic insulin signaling and stimulates production of apolipoprotein B-containing lipoproteins. *Am. J. Physiol. Gastrointest. Liver Physiol.* **297**: G323–332.
28. Repa, J. J., K. E. Berge, C. Pomajzl, J. A. Richardson, H. Hobbs, and D. J. Mangelsdorf. 2002. Regulation of ATP-binding cassette sterol transporters ABCG5 and ABCG8 by the liver X receptors alpha and beta. *J. Biol. Chem.* **277**: 18793–18800.
29. Yu, L., J. York, K. von Bergmann, D. Lutjohann, J. C. Cohen, and H. H. Hobbs. 2003. Stimulation of cholesterol excretion by the liver X receptor agonist requires ATP-binding cassette transporters G5 and G8. *J. Biol. Chem.* **278**: 15565–15570.
30. Sehayek, E., and S. L. Hazen. 2008. Cholesterol absorption from the intestine is a major determinant of reverse cholesterol transport from peripheral tissue macrophages. *Arterioscler. Thromb. Vasc. Biol.* **28**: 1296–1297.
31. Duval, C., V. Touche, A. Tailleux, J. C. Fruchart, C. Fievet, V. Clavey, B. Staels, and S. Lestavel. 2006. Niemann-Pick C1 like 1 gene expression is down-regulated by LXR activators in the intestine. *Biochem. Biophys. Res. Commun.* **340**: 1259–1263.
32. Kruit, J. K., A. K. Groen, T. J. van Berkel, and F. Kuipers. 2006. Emerging roles of the intestine in control of cholesterol metabolism. *World J. Gastroenterol.* **12**: 6429–6439.
33. Kruit, J. K., T. Plösch, R. Havinga, R. Boverhof, P. H. Groot, A. K. Groen, and F. Kuipers. 2005. Increased fecal neutral sterol loss upon liver X receptor activation is independent of biliary sterol secretion in mice. *Gastroenterology.* **128**: 147–156.
34. van der Veen, J. N., T. H. van Dijk, C. L. Vriens, H. van Meer, R. Havinga, K. Bijsterveld, U. J. Tietge, A. K. Groen, and F. Kuipers. 2009. Activation of the liver X receptor stimulates trans-intestinal excretion of plasma cholesterol. *J. Biol. Chem.* **284**: 19211–19219.
35. van der Velde, A. E., C. L. Vriens, K. van den Oever, C. Kunne, R. P. Oude Elferink, F. Kuipers, and A. K. Groen. 2007. Direct intestinal cholesterol secretion contributes significantly to total fecal neutral sterol excretion in mice. *Gastroenterology.* **133**: 967–975.
36. Fu, L., L. M. John, S. H. Adams, X. X. Yu, E. Tomlinson, M. Renz, P. M. Williams, R. Soriano, R. Corpuz, B. Moffat, et al. 2004. Fibroblast growth factor 19 increases metabolic rate and reverses dietary and leptin-deficient diabetes. *Endocrinology.* **145**: 2594–2603.